Fracture behaviour of WC-Co hardmetals with WC partially substituted by titanium carbide

M. Szutkowska[1], M. Boniecki[2], S. Cygan[1], A. Kalinka[1], M. L. Grilli[3], S. Balos[4]

[1] Institute of Advanced Manufacturing Technology, Cracow, Poland
[2] Institute of Electronic Materials Technology, Warsaw, Poland
[3] ENEA Energy Technology Department, Rome, Italy
[4] Faculty of Technical Sciences, Novi Sad, Serbia
E-mail: szutkows@ios.krakow.pl

Abstract

The addition of various amounts of $TiC_{0.9}$ phase in the range from 5wt.% to 20wt.% substituting WC phase was applied in WC-Co hardmetals with 9.5 wt.% bonding cobalt phase. The hardmetals were consolidated using Hot Isostatic Pressing (HIP) method at temperature of 1573K and pressure of 1500 atm. The plain strain fracture toughness has been determined from 3PB test on a pre-cracking single edge notched beam (SENB) specimen. The indentation fracture toughness with Vickers cracks for comparison was also measured, which changed from 12 to 9.0 $MPa \cdot m^{1/2}$. The amount of the $TiC_{0.9}$ phase affected the mechanical and physical properties: Vickers hardness from 12.5 to 14.0 GPa, Young's modulus from 550 to 460 GPa, density from 13.1 to 9.6 g/cm^3, friction coefficient from 0.24 to 0.45, fracture toughness from 16.8 to 11.0 $MPa \cdot m^{1/2}$. Scanning electron microscopy (SEM), X-ray and electron diffraction phase analysis were used to examine the WC-Co hardmetal with addition of the $TiC_{0.9}$ phase. For comparison, physical and mechanical properties of the WC-Co hardmetals before modification were tested.

Keywords: Hardmetals, sintering HIP, fracture toughness, Palmqvist cracks, titanium carbide

1. INTRODUCTION

Hardmetals or cemented carbides (sometimes less accurately called sintered carbides) are among the most commonly and most frequently used tool materials produced by powder metallurgy. The hardmetals are used to designate a metal matrix composite constituted by hard ceramic particles, normally WC, into the metallic matrix [1]. Now more than 90% of all WC-hardmetals utilize Co as the preferred binder metal with contents between 6 and 25 wt.%. The apparent superiority of cobalt, relatively to other binders, is related to its best comminution characteristics in milling, superior wettability for WC, higher solubility of WC in cobalt at sintering temperatures and excellent properties [2]. Cobalt is a ferromagnetic metal with a hcp

structure as the most stable phase at room temperature. It undergoes a phase transition from hcp into a fcc structure at 450 °C. The reasons for the dominant role of Co are also some unique properties of Co and the W–C–Co ternary system [3]. As a hard ceramic phase in WC-Co hardmetals are commonly used tungsten carbides (WC) because of their readily wettability for Co, ultimate compression strength of about 2.7 GPa, high melting point at 2870°C, extremely large Young's modulus of approximately 530-700 GPa and very good thermal conductivity of 110 W·m^{-1}K^{-1}. Tungsten carbide is very hard, ranking about 9 on Mohs scale, and with a Vickers hardness of around 26.0 GPa [4]. WC and Co form a pseudo-binary eutectic in a three component system (W, C and Co). The phase diagram also shows that there are so-called η-carbides with composition (W,Co)$_6$C that can be formed and the brittleness of these phases makes control of the carbon content in WC-Co cemented carbides important [5]. If the processing conditions are such that the carbon balance is either too high or too low then other phases are present in the structure, *i.e.* graphite if the C is high and eta-phase (an M$_6$C or M$_{12}$C, where M is generally Co$_n$W$_n$) if the C content is low. The structure of two phases WC-Co hardmetals is defined by three key parameters: grain size of the WC phase, volume fraction and composition of the Co binder phase [6]. In WC-Co hardmetals the tungsten carbides are commonly used in quantities ranging from 75 to 94 wt.%. Such a characteristic structure for hardmetals, with the presence of a ductile bonding phase and a hard and brittle carbide phase, gives combination in one material of contrasting features like: high wear resistance and hardness with high strength and good ductility. The hardmetals have the potential to change its composition so that the resulting physical and chemical properties ensure maximum resistance to wear, deformation, fracture, corrosion, and oxidation. Transverse rupture strength improves with increasing cobalt content up to a maximum of 20±5 wt.% Co. The maximum strength depends strongly on the variables, such as carbide grain size. The most important properties of the hardmetals used for mining tools are wear resistance and toughness. These properties strongly depend on content of the Co binder phase (Fig.1) [7].
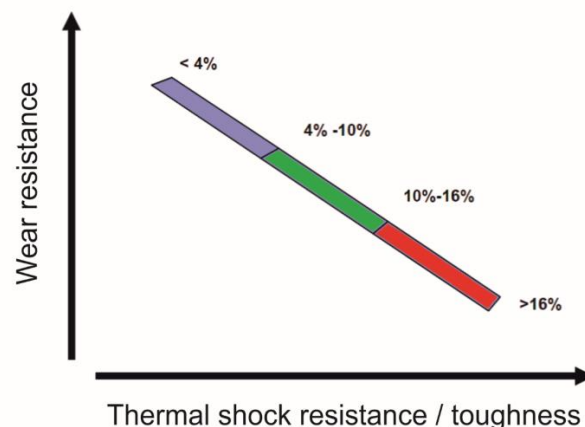

Fig.1. Wear resistance as a function of thermal shock resistance/toughness of the WC-Co hardmetals with various content of cobalt.

During the wear or fatigue processes hardmetals produce fracture from crack-like defects that develop in service. The plane strain fracture toughness of the hardmetals is represented by its critical stress intensity factor K_{IC}. Consequently, fracture toughness is an important parameter

that influences the residual strength of hardmetal components. The fracture toughness depends on content of cobalt and this property increases with an increase in the cobalt content, and with increased WC grain size (Fig.2) [7].
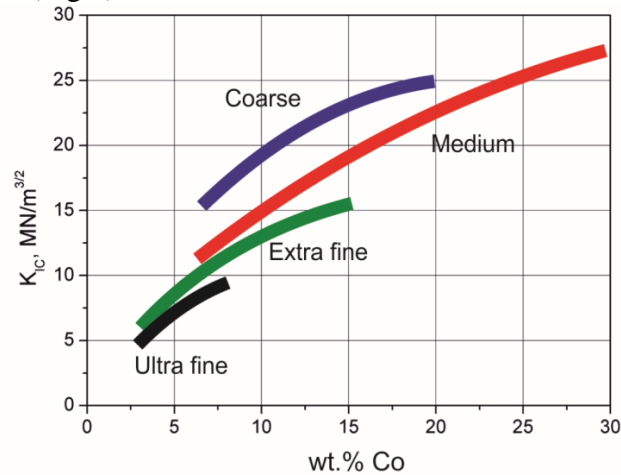

Fig.2. Plain strain fracture toughness (K_{IC}) as a function of cobalt content for different grain sizes.

Measurement of the plain strain fracture toughness for the hardmetals is difficult because there is no agreed standard test method for obtaining accurate values of K_{IC}. This is particularly important for materials with K_{IC} values greater than about 15 MN m$^{-3/2}$ that are difficult to pre-crack. Typical values of plane strain fracture toughness lie in the range 7 - 25 MN m$^{-3/2}$. These values are much higher than for similar hard materials like oxide ceramics which have fracture toughness of 3 - 7 MN m$^{-3/2}$ [6, 8]. ISO Standard [9] gives possibility to determine the Palmqvist toughness by so called the indentation fracture (IF) tests which is widely used to assess the toughness of hardmetals only for small amounts of material and allows to omit the difficulties of pre-cracking conventional toughness test-pieces. But due to particularly sensitivity to the test-piece preparation, the procedure requires re-examination for very fine grained hardmetals. A method commonly used for determining the plane strain fracture toughness of the hardmetals bases on pre-cracking conventional toughness test-pieces with notch prepared in different way (wedge indentation and fatigue SEPB specimen, beam with notch-SENB, Single Edge V-notched Beam-beam containing notch with sharpened tip diamond honed, Chevron Notched Beam-CNB and Chevron Notched Short Rod–CNSR) in the three point bending test (3PB) [6]. Unusual combinations of otherwise quite different components led to permanent technical acceptance of these materials since their discovery. Currently, tungsten carbide products are used in various industrial sectors; nearly 67% of the total hardmetals production is dedicated to cutting tools, about 13% for mining, oil extraction and tunneling, and 11% and 9% for wood and construction respectively [10].   But the WC-Co hardmetals contains tungsten carbide (WC) and cobalt (Co), both of which are defined by the EU as critical and, in the case of cobalt, dangerous to health [11,12]. The EU critical materials list contains those substances of significance to the EU economy but whose availability is at great risk, and are mostly non-renewable. Due to the significant growth of price, particularly in the recent years, of WC-Co hardmetals blends, the chemical composition of WC-Co hardmetals has been changed to reduce the WC content and substitute it with other ceramic components. It is also significant that 85%

of the world's total tungsten production is located in China, and this undoubtedly has an impact on the continuous increase in product prices [13,14]. Because titanium has a much lower risk of supply than tungsten in terms of its reserves and distribution, cubic carbides as TiC partially substituted for the WC is a good solution. Titanium carbide, with a very high melting temperature of $3065^{o}C$, has excellent properties such as: high Vickers hardness 28-32 GPa, Young's modulus of 448-451 GPa, low density of 4.94 g/cm^3, good high-temperature strength, and good corrosion resistance [15]. Additionally, no detrimental new phase is formed except that W diffuses into the TiC lattice to form a (Ti,W)C solid solution according to the TiC-W binary alloy diagram [16]. Partial replacement of WC by cubic TiC improved the high temperature strength, however, no effect on the mechanical properties was investigated [17]. Modification of WC-Co hardmetals towards the partial substitution of tungsten carbide (WC) by addition of TiC phase was the main goal of this work. This requires the change in technology of new materials by varying the pressure and temperature of sintering.

2. Experimental Procedure

A starting material was commercially available. Mixture of WC-Co powders signed as YK15.6 was delivered by the Chinese producer Chongy and Zhangyuan Tungsten Co. Ltd. According to the certificate of quality the WC-Co mixture contained 9.5 wt.% of cobalt, density of 14.57 g/cm^3 and Rockwell hardness 87.6 HRA. The grain size of the WC-Co mixture (YK15.6) was measured with the Shimadzu SA-CP3 type equipment. Density of powder was determined using AccPyc 1340 helium pycnometer, manufactured by Micrometrics Inc. The powder mixture, of 14,59 g/cm^3 density was 3.74 µm in average grain size (median), 3.53 µm in modal value and 0.730 m^2/g in surface development. The $TiC_{0.9}$ powder, of 4.93 g/cm^3 density, was 4.46 µm in average grain size (median), 15.0 µm in modal value and 1.763 m^2/g in surface development. This powder was processed by the relatively low-cost Self Propagating High Temperature Synthesis (SHS) method at the Faculty of Materials Science and Ceramics of the AGH University of Science and Technology. SEM micrographs of tested powders are presented in Fig. 3.
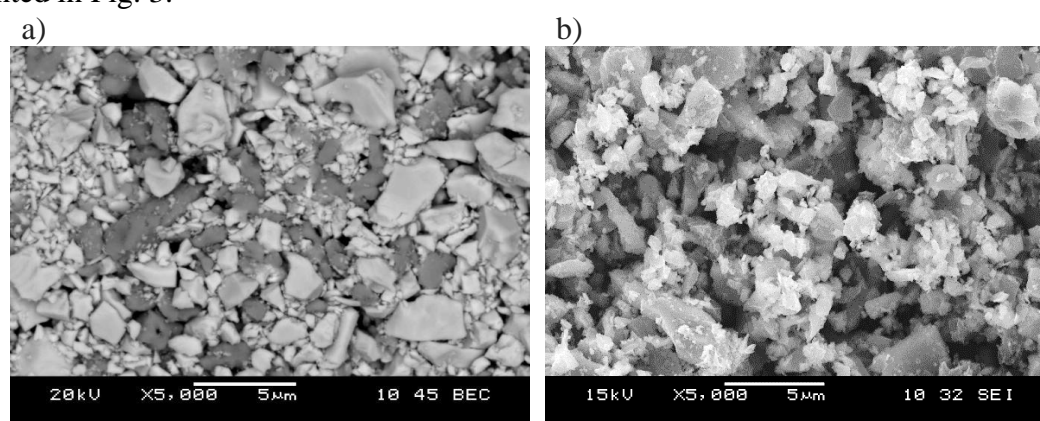
a)   b)

Fig. 3. SEM micrographs of tested powders: a) WC-Co; b) $TiC_{0.9}$

Mixture of the WC-Co powders with addition of the $TiC_{0.9}$ phase in the range from 5wt.% to 20wt.% substituting WC phase was prepared in planetary ball mill of Pulverisette 6 mono, produced by Fritsch, through 2 hours with presence of acetone as lubrication medium. 250 ml

WC milling bowl with of 5 mm in diameter WC millers was used. Green bodies were consolidated using Hot Isostatic Pressing (HIP) method at the temperature of 1573K and pressure of 152 MPa in GONAR Company. Specimens with size of 5.0x6.5x20 mm were used for various tests. After sintering specimens were lapped on a cast iron disk, ground with DIA-Pro type diamond abrasive (size of diamond grains about 9 μm) and polished with a OP-S type diamond abrasive (size of diamond grains about 0.04 μm). Following physical and mechanical properties were measured: density ρ, Young's modulus E, friction coefficient μ, Vickers hardness HV, plane strain fracture toughness K_{IC} and indentation fracture toughness $K_{IC(HV)}$. The density was determined hydrostatically, by weighing the specimen in air and in distilled water according to PN-ENISO standard [18]. The hardness was measured by the Vickers method under the load of 294.3 N, using a Future Tech FLC-50VX Vickers hardness tester. For each sample, five indentations were done. Young's modulus of the composites was determined with using a Panametrics Epoch III ultrasonic flaw detector. The measurements were based on the transition velocity of the ultrasonic waves through the sample. The velocities of transversal and longitudinal waves were designated as the ratio of the sample thickness and the relevant transition time. Because, the error in the thickness measurements was ±0.01 mm and in the time-of-flight measurements (±1 ns), the resulting error in the ultrasonic velocity was about 1%. Constantly, the error of Young's modulus measurement has obtained the value of 2%. Calculations were made using the formula:

$$E = \rho C_T^2 \frac{3C_L^2 - 4C_T^2}{C_L^2 - C_T^2} \qquad (1)$$

where: C_L — velocity of the longitudinal wave and C_T — velocity of the transversal wave, ρ-density of the material.

Plane strain fracture toughness, K_{IC} was a value obtained from tests on a specimen with a well-defined geometry of crack. Fracture toughness was assessed by means of the conventional method (3PB) on pre-cracked SENB (Single Edge Notched Beam) specimens with 1.5 mm × 4.0 mm × 15.0 ± 0.1 mm dimensions An initial notch 0.9 mm deep was produced by a diamond saw (thickness 0.20 mm) and then the notch tip was pre-cracked with a thin diamond saw(thickness 0.025mm). The total initial notch length was approximately 1.1 mm. The relationship $K_{IC}= f(c)$ is given by the Eqs. (2, 3).

$$K_{IC} = 1.5 \frac{P_c S}{W^2 B} Y c^{1/2} \qquad (2)$$

$$Y = \frac{\sqrt{\Pi}}{(1-\beta)^{\frac{3}{2}}} \left[0.3738\beta + (1-\beta) \sum_{i,j=0}^{4} A_{ij}\beta^i \left(\frac{W}{S}\right)^j \right] \qquad (3)$$

where: P_c—critical load, S—support span, W—width and B—specimen thickness, Y — geometric function, c — crack length, β — c/W and A_{ij} is the coefficients given by Fett [19].

Both the Palmqvist and the median/radial cracks propagating from the corner of the Vickers hardness indentation provide base to determination the indentation fracture toughness $K_{IC(HV)}$.

Relation between the fracture toughness and the ratio of cracks to indent size at the condition $c/a \geq 2.5$ is expressed by the equation (4) [20,21]:

$$(K_{IC} \varphi /H a^{1/2}) (H/E \varphi)^{2/5}= 0.129 (c/a)^{-3/2} \qquad (4)$$

where: K_{IC} is the critical stress intensity factor, φ is the constrain factor, H is the Vickers hardness, E is the Young's modulus, a-half of indent diagonal.

The right side of the equation (4) is equal to $0.035 (c/a)^{-1/2}$ for the Palmqvist cracks (Fig.4).
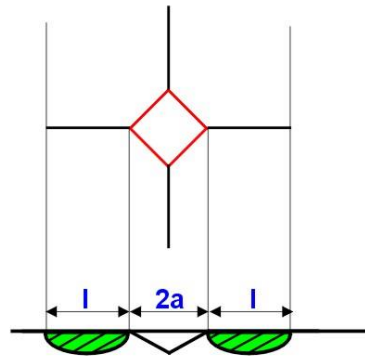

Fig. 4. Palmqvist cracks formed during an indentation toughness test.

The friction coefficients, in sliding contact with a WC ceramic ball (the ball's roughness *Ra* was 0.05 μm), were determined in ball-on-disk tests at loading 25N, using a CETR UMT-2MT universal mechanical tester (USA). The X-ray diffraction patterns were obtained by using a PANalitycal Empyrean diffractometer with copper radiation (λCu Kα = 1.5406 Å). The phase analysis was carried out with using ICDD (PDF-4+ 2016) files. The microstructure investigations were performed using a Jeol JSM-6460LV scanning electron microscope.

3. Results and Discussion

 Table 1 shows the results of the change of selected physical and mechanical properties for the WC-Co/TiC$_{0.9}$ composites with various amount of TiC$_{0.9}$. For comparison, values of tested properties for the hardmetal without addition of TiC$_{0.9}$ phase (H0) are also given.

Table.1. Selected physical and mechanical properties of tested WC-Co/TiC$_{0.9}$ hardmetals

Samples	Sample symbol	Vickers hardness HV [GPa]	Young's modulus E [GPa]	Density ρ [g/cm^3]
WC-Co +5wt%TiC	H5	12.7±0.2	549±20	13.09±0.0
WC-Co +10wt%TiC	H10	13.1±0.2	519±20	11.81±0.02
WC-Co +20wt%TiC	H20	13.9±0.2	458±20	9.60±0.03
WC-Co	H0	9.6±0.15	542±20	13.52±0.02

Mechanical and physical properties of tested hardmetals depend on the amount of the TiC$_{0.9}$ phase. The Vickers hardness *HV* increased from 12.7 to 13.9 GPa, Young's modulus *E* decreased from 549 to 458 GPa and density ρ from 13.09 to 9.60 g/cm^3 when weight percentage

of the $TiC_{0.9}$ phase increased from 5 to 20 wt%, respectively. The reduction in the density of WC-Co/ $TiC_{0.9}$ composites resulted with a five times lower $TiC_{0.9}$ density compared to the WC phase. For hardmetals with the highest percentage of $TiC_{0.9}$ (H20) phase substituting the WC phase, the increase in the Vickers hardness in comparison to WC-Co hardmetals (H0) was about 40 %. The most similar values of the Young modulus, density and Poisson ratio to the WC-Co hardmetal were obtained for the hardmetals with the smallest content of $TiC_{0.9}$ (H5). In Table 2 the results of the fracture toughness values for the WC-Co/$TiC_{0.9}$ hardmetals with various amount of $TiC_{0.9}$ and for WC-Co hardmetal without addition of $TiC_{0.9}$ phase (H0) were given.

Table.2. Fracture toughness of the WC-Co/$TiC_{0.9}$ and the WC-Co hardmetals

Specimens	**H5**	**H10**	**H20**	**H0**
Fracture toughness $K_{(IC)}$ [MPa·m$^{1/2}$]	16.8	14.0	11.1	18.5
Indentation fracture toughness $K_{IC(HV)}$ [MPa·m$^{1/2}$]	12.0	10.9	9.0	–

The plane strain fracture toughness, K_{IC} decreased with $TiC_{0.9}$ addition. It was a result of increasing the Vickers hardness of the WC-Co/$TiC_{0.9}$ hardmetals. There was a general inverse trend of the hardness against the fracture toughness.The plane strain fracture toughness of the WC-Co/5%wt.$TiC_{0.9}$ (H5) exhibits the highest value similar to the plane strain fracture toughness of WC-Co hardmetal. The indentation fracture toughness, $K_{IC(HV)}$ shows the same dependence on content of the $TiC_{0.9}$ phase in comparison to the plane strain fracture toughness, K_{IC}. It should be noted that values of the indentation fracture toughness, $K_{IC(HV)}$ are lower about 20-30% than the plane strain fracture toughness, K_{IC} determined on the basis 3PB test. The Palmqvist cracks at the corner of the Vickers indent on the specimen's surface and on the fracture of the WC-Co/$TiC_{0.9}$ hardmetal are presented in Fig.5.
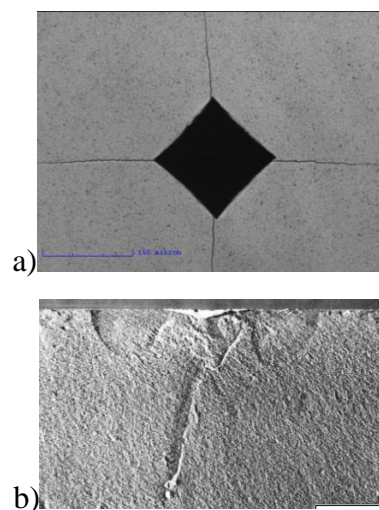

Fig.5. The Palmqvist cracks at the corner of the Vickers indent: a) surface view ; b) fracture view

At low values of Vickers hardness for WC-Co was difficult to determine indentation fracture toughness because of short, deformed cracks which make it difficult to measure the crack

length. Friction coefficient of the WC-Co/TiC$_{0.9}$ was within the range from 0.24 to 0.45 for hardmetals with 5%wt. and 20%wt. TiC$_{0.9}$, respectively, Fig. 6.
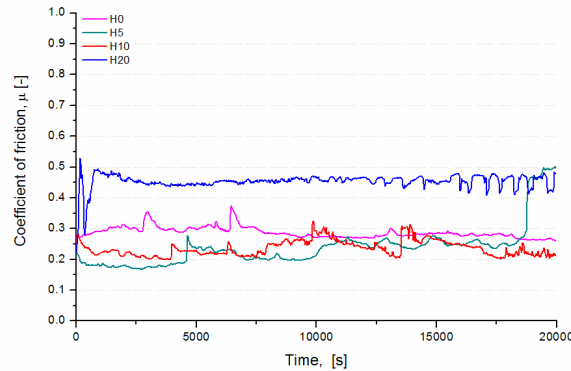

Fig.6. Friction coefficient of the WC-Co/TiC$_{0.9}$ hardmetals with various content of the TiC$_{0.9}$ phase and WC-Co hardmetal (H0).

The SEM microstructure of the WC-Co hardmetal and WC-Co/TiC$_{0.9}$ hardmetals containing an addition of 10% and 20%wt. TiC$_{0.9}$ consolidated using the HIP method is shown in figure 7. The distribution of both types of carbide particles with different shape is homogeneous. Based on the quantitative analysis of elements EDS distributed on the WC-Co/TiC$_{0.9}$ hardmetals with 10 and 20 wt.% (H10, H20) surface, presence of the: α_1WC; α_2WC; β(Ti,W)C, β'(Ti,W)C and γCo phases were observed (Fig.7).
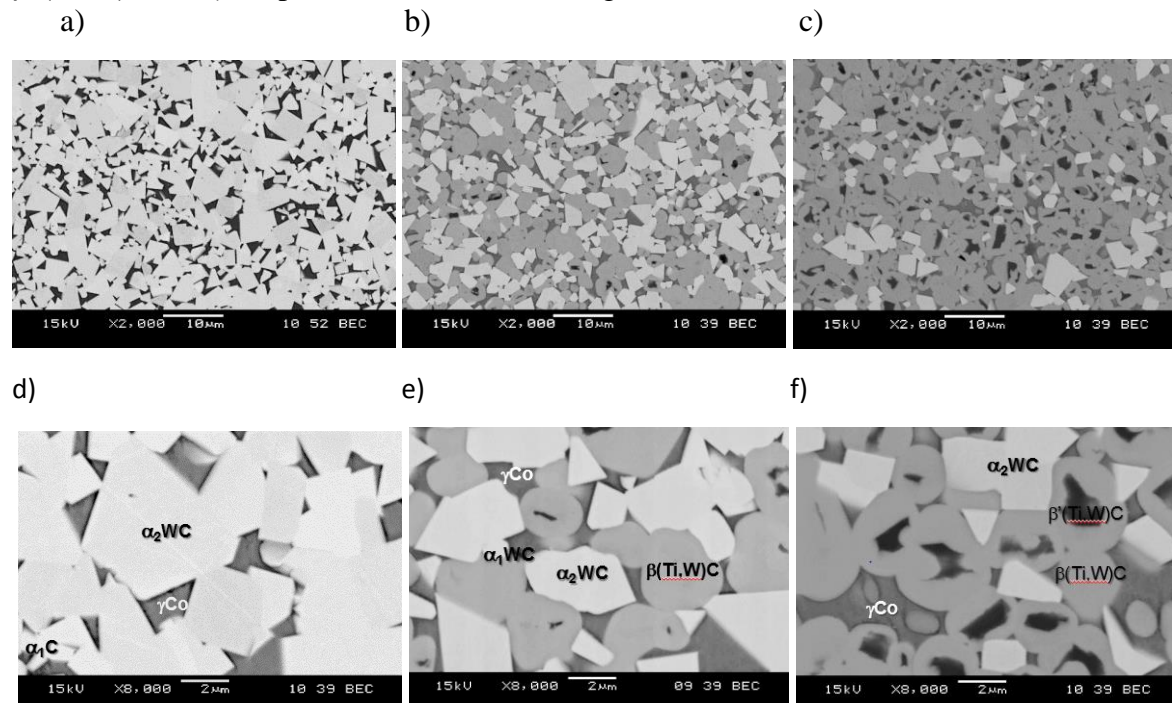

Fig.7. SEM micrograph of tested hardmetals at various magnification 2000 (a,b,c) and 8000 d,e,f): a, d) WC-Co ; b, e) WC-Co/10%wt.TiC$_{0.9}$; c, f) WC-Co/20%wt.TiC$_{0.9}$

SEM microstructure observations of the WC-Co hardmetal revealed the existence of the fine, rounded grains of the α_1WC (secondary solid solutions Co in WC non-recrystallized during

sintering), large with geometric shape, regular grains of the α_2WC phase (secondary solid solutions Co in WC recrystallized during sintering) and γCo phase (solid solution of W in Co). Addition of the $TiC_{0.9}$ reveals the new phases in spherical shape, carbides of titanium and tungsten : $\beta(Ti,W)C$ – carbide of Ti and W enhanced in W and $\beta'(Ti,W)C$ –carbide of Ti and W depleted in W with higher concentration of Ti. The $\beta'(Ti,W)C$ cores (dark) are surrounded by a $\beta(Ti,W)C$ grains (grey). The $\beta(Ti,W)C$ phases exist in the chain forms. Amount of the $\beta'(Ti,W)C$ phase increase with increasing of the $TiC_{0.9}$ phase in WC-Co hardmetals. X-ray diffraction of the WC-Co/10%wt.$TiC_{0.9}$ hardmetal which confirms the results of SEM microstructure observations is presented in Fig.8.
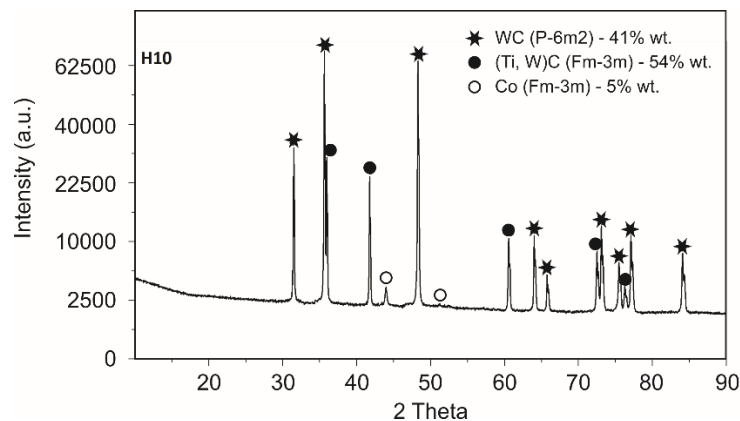

Fig.8. The X-ray diffraction of the WC-Co/10%wt.$TiC_{0.9}$ hardmetal

X-ray diffraction curves obtained from the WC-Co/10%wt.$TiC_{0.9}$ (H10) hardmetal reveal three basic phases: WC of the highest peak intensities due to its highest fraction, then Co and (Ti,W)C with increasing peak intensity when $TiC_{0.9}$ fraction increases from 5 to 20 wt.%. No intermediate phases were observed.

4. Conclusion

➢ Mechanical and physical properties of tested hardmetals depend on the amount of the $TiC_{0.9}$ phase substituted tungsten carbide in the WC-Co hardmetals.

➢ Hardmetal with the highest percentage of $TiC_{0.9}$ (H20) phase substituting the WC phase, reveal about 40% increase in the Vickers hardness in comparison to WC-Co hardmetal (H0).

➢ The inverse trend of the Vickers hardness against fracture toughness is observed.The plain strain fracture toughness of WC-Co/$TiC_{0.9}$ with 5%wt. $TiC_{0.9}$ (H5) exhibits the highest value similar to the fracture toughness of the WC-Co hardmetal.

Acknowledgments

References

[1] Ettmayer P 1989 Annu. Rev. Mater. Sci. 19 145-64
[2] Penrice TW 1988 Carbide Tool J. 20/4 12–15
[3] Fernandes C M and Senos A M S 2011 Int. Journal of Refractory Metals and Hard Materials 29 405–418
[4] Groover M P 2010 John Wiley & Sons   135
[5] Ettmayer P and Lengauer P W 1994 John Wiley & Sons
[6] Roebuck B, Gee M, Bennett E G and Morrell R Mechanical Tests for Hardmetals. Measurement Good Practice Guide No. 20. NPL England
[7] Understanding Cemented Carbides. SANDVIK Hard Materials. Destiny Tool. The mark of performance. http://www.destinytool.com/carbide-substrate.html
[8] Szutkowska M 2001 Advances in strength properties testing of sintered tool materials. Proceedings of the European Congress and Exhibition on Powder Metallurgy PM, Nice vol 2 pp 454-460
[9]   International Standard IOS 28079:2009 (E) Hardmetals - Palmqvist toughness test.
[10] Houping Z L W 2009 Cemented Carbide 26/2 pp 122-127
[11] Report On Critical Raw Materials For The European Union. Report of the Ad hoc Working Group on defining critical raw materials May 2014. http://www.catalysiscluster.eu/wp/wp-content/uploads/2015/05/2014_Critical-raw-materials-for-the-EU-2014.pdf
[12] Grilli ML, Bellezze T, Gamsjäger E, Rinaldi A, Novak P, Balos S, Piticescu RR, Ruello ML 2017 Solutions for Critical Raw Materials under Extreme Conditions: A Review, Materials, 10, 285.
[13] Silberglitt R, Bartis J T, Chow B G, An D L and Brady K 2013 Critical Materials. Present Danger to U.S. Manufacturing. RAND. National Defense Research Institute. Library of Congress Cataloging-in-Publication Data. ISBN: Copyright 2013 RAND Corporation.
[14] Ishida T, Moriguchi H and Ikegaya A 2011 Sei Technical Review 73   pp 52-55
[15] Bauccio M Ed. 1994 ASM Engineered Materials Reference Book, Second Edition, ASM International, Materials Park, OH
[16] Lipatnikov V N, Rempel A A and Gusev A I 1997 Int. J. Refract. Met. Hard Mater. 15 pp 61-4.
[17] Baratti C, Garcia J, Brito P and Pyzalla A R 2009 Int. J. Refract. Met. Hard Mater. 27 pp 768-776.
[18] PN-EN ISO 3369:2010E Impermeable sintered metal materials and hardmetals - Determination of density.
[19] Fett T 1991 Eng. Fract. Mech. 40/3 pp 683–686.
[20] Niihara K. et al. 1982 Communications of the Amer. Ceram. Soc., C-116
[21] Szutkowska M, Boniecki M 2010 Journal of Optoelectronics and Advanced Materials vol. 12/2 pp 301– 308